

## Fabrication and Characterization of Metallic Copper and Copper Oxide Nanoflowers

\*H. S. Virk

Nanotechnology Laboratory, DAV Institute of Engineering and Technology (DAVIET)  
Kabir Nagar, Jalandhar-144008, India.  
Email: \*hardevsingh.virk@gmail.com

### ABSTRACT

Copper nanoflowers have been fabricated using two different techniques; electro-deposition of copper in polymer and anodic alumina templates, and cetyltrimethyl ammonium bromide (CTAB)-assisted hydrothermal method. Scanning Electron Microscope (SEM) images record some interesting morphologies of metallic copper nanoflowers. Field Emission Scanning Electron Microscope (FESEM) has been used to determine morphology and composition of copper oxide nanoflowers. X-ray diffraction (XRD) pattern reveals the monoclinic phase of CuO in the crystallographic structure of copper oxide nanoflowers. There is an element of random artistic design of nature, rather than science, in exotic patterns of nanoflowers fabricated in our laboratory.

**Keywords:** nanoflowers, electrodeposition, electrolytic cell, polymer template, anodic alumina template, nanopores, hydrothermal method, morphology, nucleation rate, stoichiometry

### 1. INTRODUCTION

During the last decade, exhaustive reviews<sup>1-4</sup> have been published on metal nanostructures. A series of various nanoflowers and nanoflower-like structures have been obtained, depending on reaction conditions, such as reagents ratio, temperature and other conditions. Nanoflower structure may consist of such more simple nanostructures, as nanorods, nanowalls, or nanowires. Current and possible applications of nanoflowers as optoelectronics devices or sensors, in catalysis, and solar cells caused a definite interest in them. Nanoflowers of almost all metals have been reported in the form of elemental nanoflowers; metal oxide nanoflowers; nanoflowers of hydroxides and oxosalts; sulphide, selenide and telluride nanoflowers; nitride and phosphide nanoflowers; nanoflowers formed by organic and coordination compounds<sup>1</sup>.

Flower-like cupric oxide (CuO) nanostructures have been prepared via cetyltrimethyl ammonium bromide (CTAB)-assisted hydrothermal method<sup>5</sup>. CTAB is a useful surfactant that has been widely used in fabricating the nanomaterials to control the morphology. Cao et al.<sup>6</sup> reported CTAB-assisted hydrothermal synthesis of CuO of various morphologies such as rod-like, spheroidal, hexahedron and other irregular structures. Cupric oxide (CuO) has potential applications in many fields, such as superconductor<sup>7</sup>, gas sensor<sup>8</sup>, catalyst<sup>9</sup>, magnetic storage media<sup>10</sup> and lithium battery<sup>11</sup>.

Author's group<sup>12-14</sup> has reported fabrication and characterization of copper nanowires and some exotic patterns of polycrystalline copper recently using electrodeposition technique of template synthesis. A comprehensive investigation is planned to exploit the industrial applications of copper nanoflowers, for example, field emission properties.

### 2. EXPERIMENTAL

There are several different methods for fabrication of nanoflowers as reported in various reviews<sup>1-4</sup>. We followed two different routes for preparation of copper nanoflowers: electro-deposition technique using template synthesis and CTAB-assisted hydrothermal method.

Electro-deposition technique used in our experiment<sup>12-14</sup> is similar in principle to that used for the electroplating process. Commercially available polycarbonate membranes (Sterlitech, USA) of 25 mm diameter with pore density of  $10^8$  pores/cm<sup>2</sup> and pore diameter of 100 nm were selected for this experiment. The main purpose of this experiment was to fabricate nanowires of copper. However, to our utter surprise, we failed in our mission and what we got was a blessing in disguise. We observed formation of some exotic patterns, including synthesis of nanoflowers.

A second set of experiments was completed using commercial anodic alumina membranes (AAM) (anodic 25 made by Whatman) having an average pore diameter of 200 nm, a nominal thickness of 60  $\mu$ m and a pore density of  $10^9$  pores/cm<sup>2</sup>, as templates.

The electrochemical cell, fabricated in our laboratory using Perspex sheets, was washed in double distilled water. A copper rod of 0.5 cm diameter was used as a sacrificial electrode (anode). The cathode consists of copper foil attached to polymer template by an adhesive tape of good conductivity. The electrolyte used had a composition of 20 gm/100ml CuSO<sub>4</sub>.5H<sub>2</sub>O + 25% of dilute H<sub>2</sub>SO<sub>4</sub> at room temperature. The inter-electrode distance was kept 0.7 cm and a current of 2mA was applied for 10 minutes. The polymer template was dissolved in dichloromethane to liberate copper nanoflowers from the host matrix. Copper nanowires were produced generally using AAM template but in

some cases, nanoflowers appeared on the periphery of template due to poor contact. The Scanning Electron Microscope (JEOL, JSM 6100) was used to record top and side views of grown nanostructures at an accelerating voltage of 20kV using different magnifications.

For hydrothermal synthesis<sup>5</sup>, analytical grade (Loba Chemicals) copper chloride dihydrate,  $\text{CuCl}_2 \cdot 2\text{H}_2\text{O}$ , and sodium hydroxide, NaOH, were used as precursors and CTAB as surfactant. All the chemicals were directly used without further purification and de-ionized water was used for preparation of solution.

In a typical synthesis, the copper chloride solution was prepared by dissolving 0.8524g (5mmol) of  $\text{CuCl}_2 \cdot 2\text{H}_2\text{O}$  in 20mL de-ionized water. Subsequently, the copper chloride solution was slowly dropped into 50mL of NaOH solution ( $3\text{mol} \cdot \text{L}^{-1}$ ) under vigorous stirring. The blue-colored precursor was obtained. 1g of CTAB (3 mmol) was added to the blue-colored precursor and stirred vigorously for 30 min at  $50^\circ\text{C}$  to ensure the complete dissolution of CTAB. This reaction solution was then transferred to a 50 mL Teflon-lined stainless steel autoclave and heated at  $150^\circ\text{C}$  for 12 h in an electric oven. After reaction, autoclave was allowed to cool to room temperature. The resulting black precipitate was centrifuged and washed thoroughly with de-ionized water and ethanol. Then the precipitate was dried in drying oven at  $50^\circ\text{C}$  for 24 h. Finally, the reaction products were calcined in a furnace at  $500^\circ\text{C}$  for 2h in an ambient air atmosphere.

### 3. RESULTS AND DISCUSSION

There is as yet no specific theory to explain exotic patterns developed during electro-deposition of copper in anodic alumina or polymer templates. A speculative explanation<sup>15</sup> is provided on the basis of over-deposition. During the growth of copper nanowires in the template pores, the current remains nearly stable until the wires arrive at the template surface. If the electro-deposition process is not stopped at this stage, the current keeps on rising very gradually leading to over-deposition of copper. The exotic patterns in the form of micro-flowers having their petals in nanometer dimension, copper buds leading to mushroom effect and double pyramid shaped copper crystals have been observed in our investigations<sup>12-14</sup>. It has also been reported<sup>16</sup> that over-deposition of copper in polymer templates may lead to formation of metallic micro-rose having petals in nanometer dimensions. Flower-like morphology of metal over-deposits has been attributed to the changes in hydrodynamic conditions due to excessive hydrogen evolution during electro-deposition process<sup>16</sup>.

During our recent experiments, we observed that the growth of nanoflowers depends upon two factors: cathode over-potential and conductivity of the cathode surface. If the conducting film is used for the cathode surface, Cu ions will tend to deposit into nanochannels of polymer template, otherwise they tend to grow laterally on the cathode surface. The deposition of copper takes place only when the potential of the cathode is lower than the equilibrium electrode potential of the electrolytic cell; hence, a certain magnitude of cathode over-potential is necessary. The relationship between the over-potentials and the nucleation rates was given by Erday-Gruz and Volmer<sup>17</sup> as follows:

$$N = a e^{-b/\eta_k^2} \quad (1)$$

Where  $N$  is the nucleation rate;  $\eta_k$  is the cathode over-potential; and  $a$  and  $b$  are constants. It can be seen that the higher the over-potential, the higher the nucleation rates of growth. At a certain optimum over-potential, nanoflower fabrication occurs.

SEM micrographs of copper nanoflowers fabricated using polymer templates are shown (Figs. 1-3). Figure 1 shows the deposition of copper in the form of flower petals. Figure 2 depicts two different shapes of copper nanoflowers. Figure 3 represents lily-like botanical plants of copper metal grown on the cathode surface. The beauty of these experiments is that no identical patterns are produced on repeating the experiment.

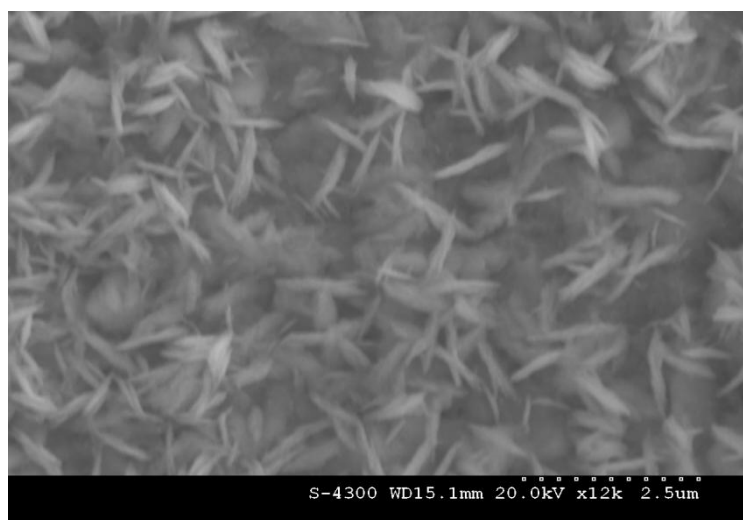


**Fig-1:** SEM micrograph of copper nanoflower petals grown in polymer template

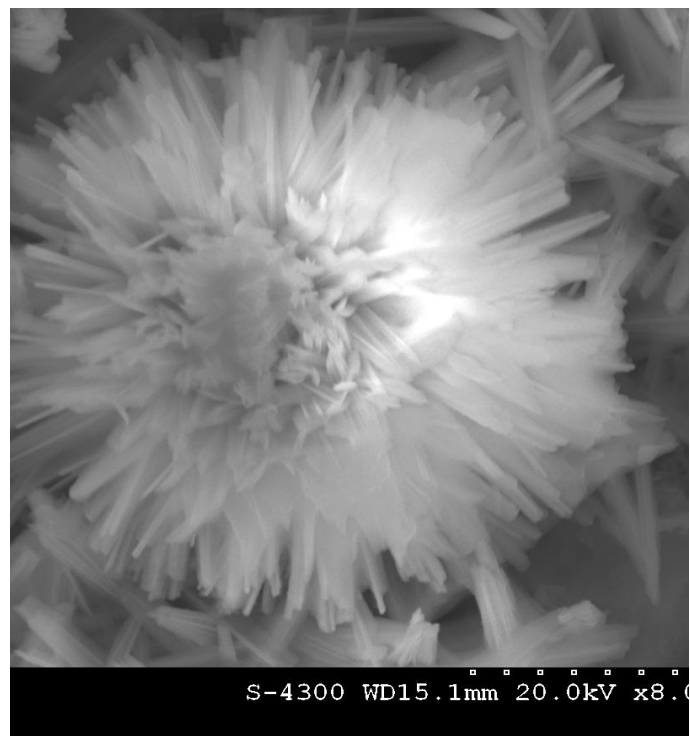
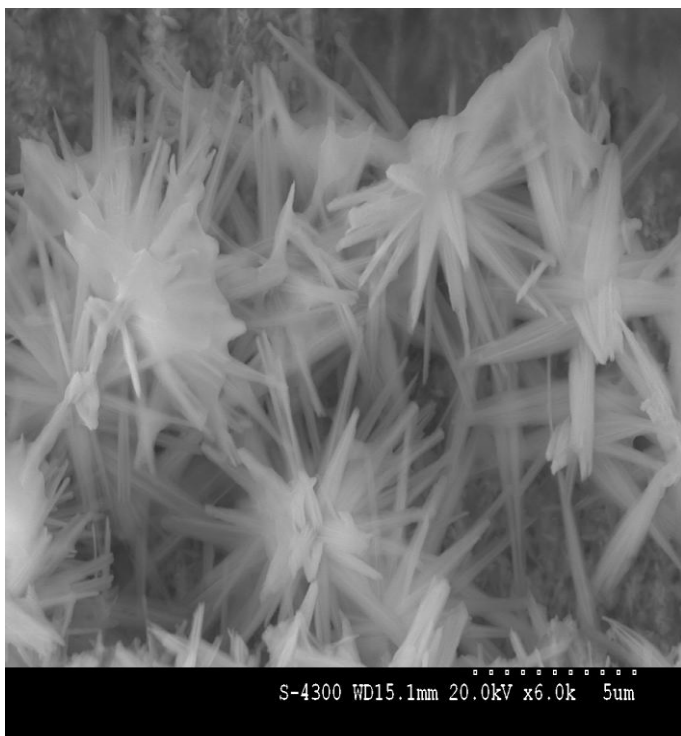


**Fig-2(a,b):** SEM micrographs of copper nanoflowers grown in polymer template



**Fig-3(a,b):** SEM micrograph of lily-like copper plants grown in polymer template

In case of anodic alumina template, copper nanowires<sup>12</sup> were grown in central region and nanoflowers in peripheral zone (Fig. 4). It shows differential deposition of copper on the cathode surface. It is difficult to determine the exact conditions under which nanoflowers are synthesized along with nanowires. Our investigations reveal that chance plays a predominant role in growth of nanoflowers. The most disturbing feature of our study is that different types of nanostructures are created under similar experimental conditions. There is an element of random artistic design in nanoflowers fabricated in our laboratory. However, there is one satisfaction that all these exotic patterns find some analogue in nature.

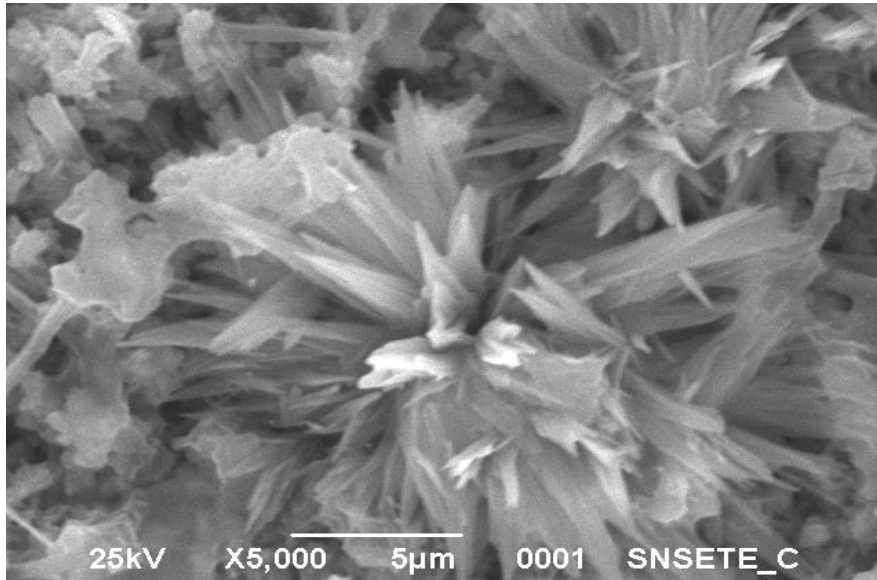


**Fig-4:** SEM micrograph of copper nanoflowers grown in anodic alumina template

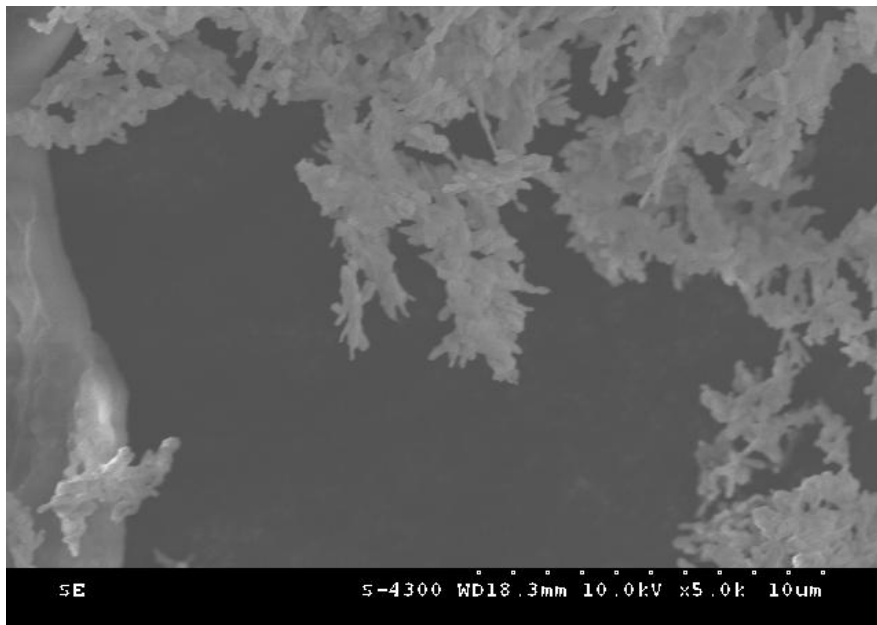


**Fig-5:** FESEM micrograph of CuO nanoflowers prepared by hydrothermal method

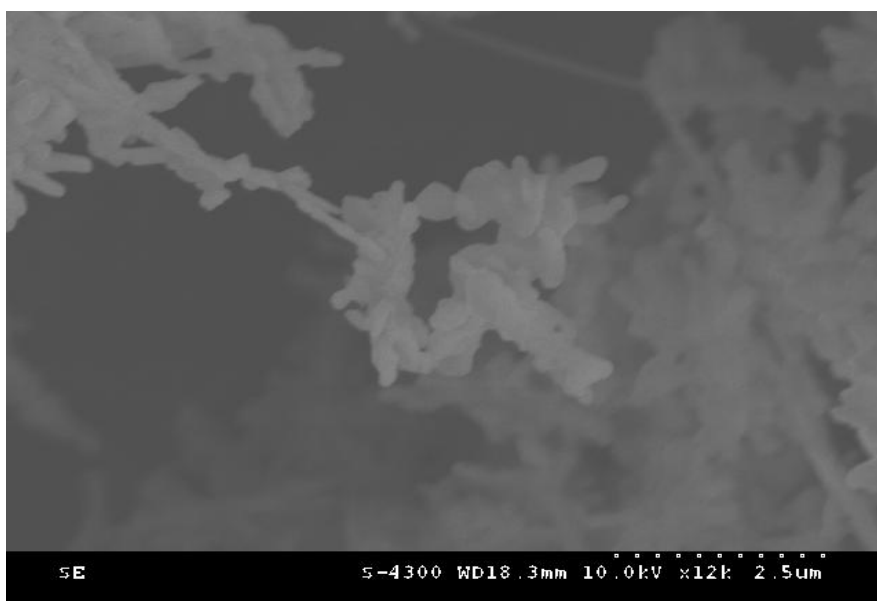


**Fig-6:** FESEM image depicting shape of CuO nanoflower by hydrothermal method

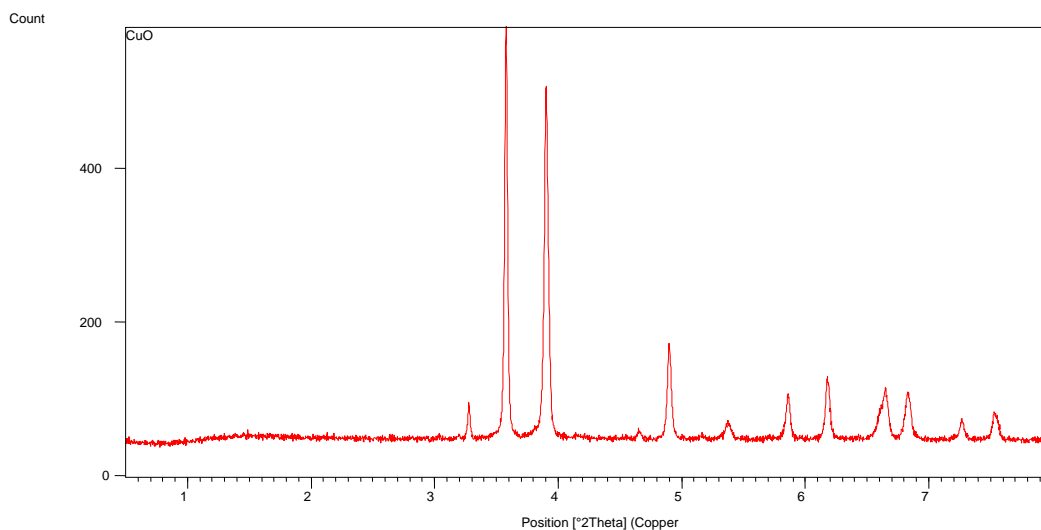


**Fig-7:** XRD spectrum of monoclinic copper oxide nanoflowers

**Table-1:** XRD spectrum peaks data of CuO nanoflowers

Pos. [ $^{\circ}2\text{Th.}$ ]	FWHM [ $^{\circ}2\text{Th.}$ ]	d-spacing [ $\text{\AA}$ ]	Rel. Int. [%]	Area [cts* $^{\circ}2\text{Th.}$ ]
32.7906	0.1338	2.73127	8.01	55.93
35.8066	0.2509	2.50784	100.00	1309.41
38.9983	0.1673	2.30963	83.89	732.34
46.5518	0.2676	1.95095	1.79	24.99
48.9563	0.1506	1.86061	22.75	178.74
53.7459	0.2342	1.70556	4.34	53.09
58.6036	0.3011	1.57524	10.74	168.78
61.7668	0.2007	1.50195	14.27	149.44
66.4776	0.2007	1.40649	12.33	129.17
68.2783	0.1673	1.37372	10.87	94.87
72.6435	0.3011	1.30156	4.59	72.17
75.2766	0.1632	1.26139	6.83	78.61

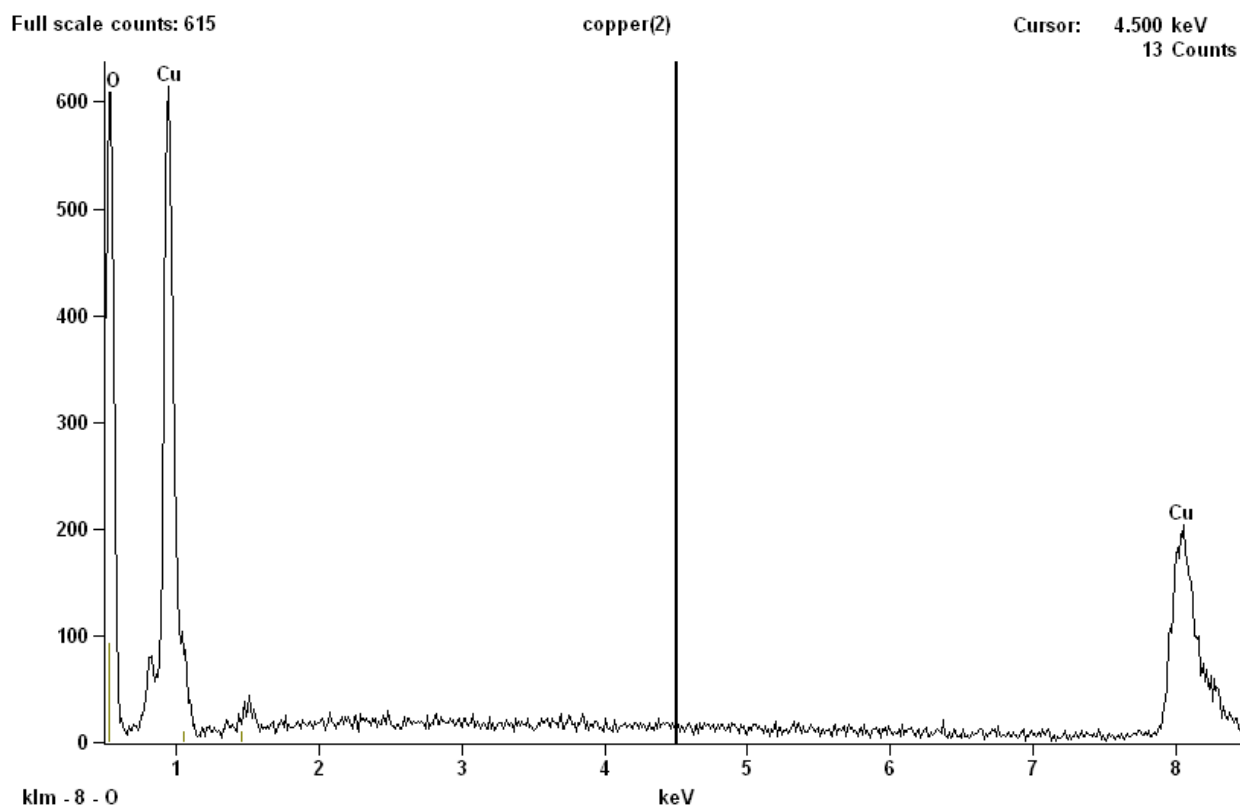


**Fig-8:** EDX spectrum of copper oxide nanoflowers prepared by hydrothermal method

**Table- 2:** Quantitative results for copper oxide nanoflowers composition

<i>ElementLine</i>	<i>Weight %</i>	<i>Weight %Error</i>	<i>Atom %</i>	<i>Atom %Error</i>
<i>O K</i>	33.60	+/- 0.73	66.77	+/- 1.44
<i>Cu K</i>	66.40	+/- 3.31	33.23	+/- 1.66
<i>Total</i>	100.00		100.00	

FESEM micrographs (Figs. 5-6) show CTAB-assisted hydrothermal synthesis of CuO nanoflowers. The explanation for CTAB-assisted hydrothermal method of CuO flowers fabrication is given by Zou et al.<sup>5</sup>. According to the literature survey, the formation mechanisms of the flower-like CuO nanostructures were different when different preparation methods were used. Yu et al.<sup>18</sup> prepared the flower-like CuO nanostructures by reaction between a Cu plate and a KOH solution at room temperature and demonstrated their field emission properties. They speculated that the nanoflower was a representative morphology of spherulite formed by radiating growth from a center or a number of centers and the  $[\text{Cu}(\text{OH})_4]^{2-}$  complexes played a key role in the growth of nanoflowers. Zhu et al.<sup>19</sup> obtained the flower-like CuO nanostructures composed of many interconnected needle-like crystallites by hydrolyzing of  $\text{Cu}(\text{OAc})_2$  solution without any surfactants. Teng et al.<sup>20</sup> synthesized the flower-like CuO nanostructures by hydrothermal process using copper threads as precursor. They investigated the influences of hydrothermal temperature and hydrothermal time on the nanostructures and reported that the formation of the flower-like structure was controlled not only by the growth thermodynamics, but also by the growth kinetics.

The crystallographic structure of copper oxide nanoflowers was investigated by X-ray diffraction analysis (XRD). The typical XRD spectrum shows 12 peaks with two major peaks at  $2\theta = 35.8066$  and  $38.9983$ , corresponding to Miller indices (111) and (200). All the peaks are compared with the standard XRD spectrum<sup>21</sup> (AMCSD Card Number: 99-101-0934 of American Mineralogist Crystal Structure Database) and a perfect matching exists between the two spectra. In comparison with standard XRD spectrum, the main peak at  $2\theta = 35.8066$  can be indexed to characteristic diffraction of monoclinic phase of CuO with cell parameters ( $a=0.4653$  nm,  $b=0.3410$  nm,  $c=0.5108$  nm). The Miller indices of all the peaks in XRD spectrum are represented by (110), (111), (200), (201), (202), (112), (020), (113), (022), (220), (311) and (222).

Energy dispersive X-ray analysis (EDX) of CuO nanoflowers was performed using the FESEM facility of Central Scientific Instruments Organization (CSIO), Chandigarh to determine their chemical composition and stoichiometry. The spectrum (Fig. 8) reveals 3 major peaks: two peaks of copper and one peak of oxygen. Table 2 reveals that the chemical composition of nanoflowers by weight percent and atomic percent are reciprocal. EDX spectrum reveals also the chemical purity of CuO nanoflowers as other trace impurities are found to be absent.

#### 4. CONCLUSIONS

Template synthesis is an elegant method for fabrication of copper nanoflowers, using anodic alumina or polymer templates. Over-deposition plays sterling role in the growth of exotic patterns of copper. CuO nanoflowers exhibit monoclinic phase and polycrystalline nature. No scientific theory is yet available to explain their exact nature. It has been discovered that nanoflowers have great potential for possible applications in nanotechnology. CuO nanoflowers have been exploited as sensor for hydrogen peroxide ( $\text{H}_2\text{O}_2$ )<sup>22</sup> and hydrazine<sup>23</sup>, as well as for optical<sup>24</sup> and field emission properties<sup>18</sup>.

#### 5. ACKNOWLEDGEMENTS

The author is grateful to Shree C. L. Kochher, Regional Director, DAV Institute of Engineering & Technology, Jalandhar and DAV Colleges Managing Committee, New Delhi for providing research grant to set up Research Centre and Nanotechnology Laboratory in Jalandhar. FESEM analysis was carried out at CSIO, Chandigarh. Author wishes to record his appreciation to Dr. Pawan Kapur, Director CSIO, Chandigarh and Dr Lalit M. Bharadwaj, Head Nanotechnology Group at CSIO for providing research facilities. Dr Inderpreet Kaur and her research team also deserve my appreciation for rendering all possible help during characterization. Mr. Mohinder Singh and Jagtar Singh at SAIF, Punjab University, Chandigarh provided all help in SEM and XRD analysis of samples, respectively, whenever I approached them. Special thanks are due to my research assistants for help in preparation of samples.

#### 6. REFERENCES

1. Kharisov, B. I., Recent Patents on Nanotechnology, (2008) 2(3): 190-200, <http://dx.doi.org/10.2174/187221008786369651>.
2. Kharissova, O. V., Kharisov, B. I., Recent Patents on Nanotechnology, (2008) 2(2): 103-119, <http://dx.doi.org/10.2174/187221008784534505>.
3. Kharissova, O. V., Kharisov, B. I., Garcia, T. H., Mendez, U. O., Synthesis and Reactivity in Inorganic, Metal-Organic and Nano-Metal Chemistry, (2009) 39: 662-684.

4. Kharisov, B. I., and Kharissova, O. V., *Ind. Eng. Chem. Res.*, (2010) 49: 11142-11160, <http://dx.doi.org/10.1021/ie1017139>.
5. Zou, Y., Li, Y., Zhang, N., Li, J., *Adv. Mater. Res.*, (2011) 152-153: 909-914, <http://dx.doi.org/10.4028/www.scientific.net/AMR.152-153.909>.
6. Kharissova, O. V., Cao, M. H., Hu, C. W., Wang, Y. H., Guo, Y. H., Guo, C. X., Wang, E. B., *Chem. Comm.*, (2003) 15: 1884-1885.
7. Schon, J. H., Dorget, M., Beuran, F. C., Zu, X. Z., Arushanov, E., Cavellin, C. D., Lagues, M., *Nature*, (2001) 414: 434-436, <http://dx.doi.org/10.1038/35106539>.
8. Tamaki, J., Shimanoc, K., Yamada, Y., Yamamoto, Y., Miura, N., Yamazoe, N., *Sensors & Actuators B*, (1998) 49: 121-130, [http://dx.doi.org/10.1016/S0925-4005\(98\)00144-0](http://dx.doi.org/10.1016/S0925-4005(98)00144-0).
9. Reitz, J. B., Solomon, E. I., *J. Am. Chem. Soc.*, (1998) 120: 11467-11478, <http://dx.doi.org/10.1021/ja981579s>.
10. Ziolo, J., Borsa, F., Corti, M., Rigamonti, A., Parmigiani, F., *J. Appl. Phys.*, (1990) 67: 5864-5866, <http://dx.doi.org/10.1063/1.345996>.
11. Gao, X. P., Bao, J. L., Pan, G. L., Zhu, H. Y., Huang, P. X., Wu, F., Song, D. Y., *J. Phys. Chem. B*, (2004) 108: 5547-5551, <http://dx.doi.org/10.1021/jp037075k>.
12. Virk, H. S., Balouria, V., Kishore, K., *J. Nano Res.*, (2010) 10: 63-67.
13. Virk, H. S., *J. Nano Sci. Nano Engg. & Applications*, (2010) 1(1):1-14.
14. Virk, H. S., *Nano Trends*, (2010) 9 (1): 1-9.
15. Gao, T., Meng, G., Wang, Y., Sun, S., Zhang, L., *J. Physics: Condensed Matter*, (2002) 14: 355-363, <http://dx.doi.org/10.1088/0953-8984/14/3/306>.
16. Kumar, S., Kumar, V., Sharma, M. L., Chakarvarti, S. K., *Superlattices and Microstructures*, (2008) 43: 324-329, <http://dx.doi.org/10.1016/j.spmi.2008.01.005>.
17. Erday-Gruz, T., Volmer, M., *Z. Phys. Chem. A*, (1930) 150: 203.
18. Yu, L. G., Zhang, G. M., Wu, Y., Bai, X., Guo, D. Z., *J. Cryst. Growth*, (2008) 310: 3125-3130, <http://dx.doi.org/10.1016/j.jcrysgro.2008.03.026>.
19. Zhu, J. W., Bi, H. P., Wang, Y. P., Wang, X., Yang, X. J., Lu, L. D., *Mater. Lett.*, (2007) 61: 5236-5238, <http://dx.doi.org/10.1016/j.matlet.2007.04.037>.
20. Teng, F., Yao, W. Q., Zheng, Y. F., Ma, Y. T., Teng, Y., Xu, T. G., Liang, S. H., Zhu, Y. F., *Sensors & Actuators B*, (2008) 134: 761-768, <http://dx.doi.org/10.1016/j.snb.2008.06.023>.
21. Downs, R. T., Hall-Wallace, M., *American Mineralogist*, (2003) 88: 247-250.
22. Gu, A., Wang, G., Zhang, X., Fang, B., *Bull. Material Sci.*, (2010) 33(1): 17-20, <http://dx.doi.org/10.1007/s12034-010-0002-3>.
23. Zhang, X., Gu, A., Wang, G., Wang, W., Wu, H., Fang, B., *Chem. Letters*, (2009) 38(5): 466-467, <http://dx.doi.org/10.1246/cl.2009.466>.
24. Luo, Y., Xia, X., Ren, Q., Li, S., Li, J., Jia, Z., *Dianzi Yuanjian Yu Cailiao (Chinese)*, (2007) 26(2): 11-13.